GENERALIZED COMPENSATION METHOD FOR NONLINEAR INDUCTANCES AND RESISTANCES REPRESENTATION IN ELECTROMAGNETIC TRANSIENTS STUDIES

M.Sc. Eng. G. Calzolari / M.Sc. Eng. C.Saldaña
Av. Millán 4016 - Montevideo
11700 URUGUAY
Phone: (005982) 47 56 05

SCOPE

This paper presents some basic principles of Generalized Compensation Method for nonlinear elements representation in power systems. A subroutine program called NONLIN,in Fortran 77 Languaje, was specially developed for this methodology, by the authors,and added to the EFEI's Electromagnetic Transients Program(Escola Federal de Engenharia de Itajuba), Brazil.
Some results of switching surges and temporary overvoltages simulated in a power system using NONLIN subroutine and other models are included.Finally a comparison was made between the obtained results from simulations and that from field tests data.

KEY WORDS

Electromagnetic transients, nonlinear resistances and inductances, compensation method.

1. INTRODUCTION

The digital simulation of electromagnetic transients in a power system is made modelling each of their components. Some of them are nonlinear,such as:surge arresters with gaps, ZnO surge arresters, reactors with saturable core, transformers, circuit breakers, etc. On account of the nonlinearity of these elements there is a system of nonlinear differential equations that describe their behavior.
Therefore, the calculation of branch currents and voltages, in the time domain, could be made in the two following ways:

a) applying numerical methods to solve the set of nonlinear differential equations.
b) modifying the linear methods in such a way to include nonlinear elements.

The last methodology is used in most digital programs of calculation because the total time solution does not increase in excess on account of the few number, in general, of nonlinear elements.
The Generalized Compensation Method, one of the modifications made in the linear methods, it's applied in this paper to model nonlinear resistances and inductances.

2. BASIC PRINCIPLE [1] [2] [6]

In this section the extension of the compensation method to N nonlinearities is described, which allows to calculate nodal voltages for the entire network at instant t_0.This procedure is applied successively at discrete intervals of time.

2.1 Generalized Compensation Method

This method is based on two theorems:
- superposition theorem
- substitution theorem

The substitution theorem states: any branch of one circuit can be substituted for other if the current and voltage drop between terminals in both of them is the same.
The most frequent use of this method consists in a substitution of one passive element of a circuit by a voltage or current source.
Figure 1 shows a scheme of the network that contains N nonlinear elements between pair of nodes: 1-1', 2-2',....., N-N'.

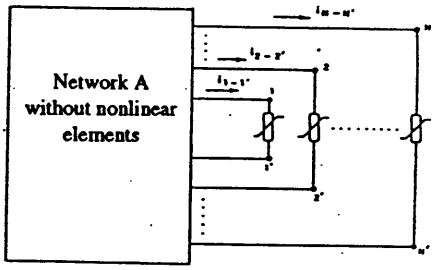

Figure 1 - Scheme of the network with N nonlinear elements

The procedure to calculate all network's nodal voltages, at instant t_0, has three stages:

First stage:
The substitution theorem states that each nonlinear element can be replaced by a current source. The values of the sources $i_{1\text{-}1'}(t_0), i_{2\text{-}2'}(t_0),.....,i_{N\text{-}N'}(t_0)$ are the currents that flow in nonlinear elements at instant t_0. This stage is shown in Figure 2.

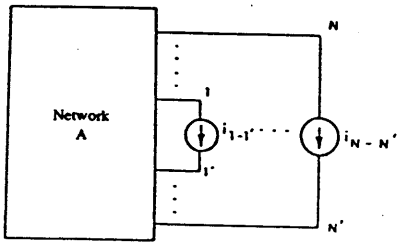

Figure 2 - Scheme of the network after the first stage

Second stage:
Nonlinear elements are removed from the original network in such a way that the remaining network only has linear elements and sources. The trapeziodal rule applied to a set of differential equations that describe the remaining network behavior allow to use nodal analysis which leads to a nodal conductance matrix.

The remainig network is reduced to a Thevenin equivalent circuit seen from pairs of nodes: 1-1', 2-2' ,....,N-N'.
For this circuit the following matricial equation can be written:

$$\begin{bmatrix} v_{1\text{-}1'}(t_0) \\ v_{2\text{-}2'}(t_0) \\ \cdot \\ \cdot \\ \cdot \\ v_{N\text{-}N'}(t_0) \end{bmatrix} = \begin{bmatrix} v^0_{1\text{-}1'}(t_0) \\ v^0_{2\text{-}2'}(t_0) \\ \cdot \\ \cdot \\ \cdot \\ v^0_{N\text{-}N'}(t_0) \end{bmatrix} - [R_{TH}] . \begin{bmatrix} i_{1\text{-}1'}(t_0) \\ i_{2\text{-}2'}(t_0) \\ \cdot \\ \cdot \\ \cdot \\ i_{N\text{-}N'}(t_0) \end{bmatrix} \quad (01)$$

where :

$v_{1\text{-}1'}(t_0),....,v_{N\text{-}N'}(t_0)$ - voltages across N nonlinear elements
$v_{1\text{-}1'}{}^0(t_0),....,v_{N\text{-}N'}{}^0(t_0)$ - open-circuit voltages across the node pairs 1-1',....,N-N'
$[R_{TH}]$ - Thevenin equivalent resistences matrix
$i_{1\text{-}1'}(t_0),.....,i_{N\text{-}N'}(t_0)$ - branch currents of N nonlinear elements

For each nonlinear element is possible to obtain a curve voltage x current, which can be given analytically or defined point-by-point. Then for the N nonlinear elements the following matricial equation can be written:

$$\begin{bmatrix} v_{1\text{-}1'}(t_0) \\ v_{2\text{-}2'}(t_0) \\ \cdot \\ \cdot \\ \cdot \\ v_{N\text{-}N'}(t_0) \end{bmatrix} = \begin{bmatrix} f_1(i_{1\text{-}1'}, t_0) \\ f_2(i_{2\text{-}2'}, t_0) \\ \cdot \\ \cdot \\ \cdot \\ f_N(i_{N\text{-}N'}, t_0) \end{bmatrix} \quad (02)$$

The equations (01) and (02) are a set of 2N nonlinear equations with 2N unknown variables:

$$v_{1\text{-}1'}(t_0) \ldots\ldots\ldots\ldots v_{N\text{-}N'}(t_0)$$
$$i_{1\text{-}1'}(t_0) \ldots\ldots\ldots\ldots i_{N\text{-}N'}(t_0)$$

If the functions f_1 , f_2....,f_N are given analytically, then a numerical method is applied to solve the systems of equations, for example Newton-Raphson method.
In this way the branch voltages and currents of N nonlinear elements at instant t_0 are calculated.

Third stage:
The superposition theorem can be applied at instant t_0, in the network of Figure 2, as shown in Figure 3.

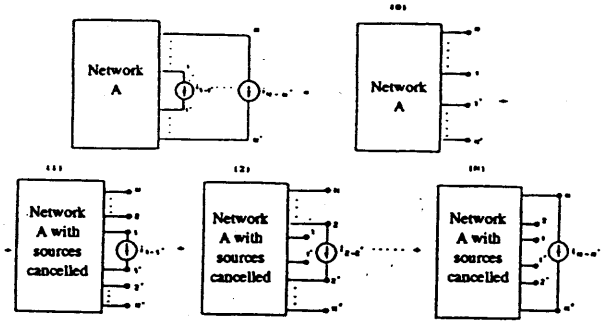

Figure 3 - Application of superposition theorem at instant t_0 in the network of Figure 2

Finally the node voltages for the entire network of Figure 1 at instant t_0, are found through the following matricial equation:

$$[v_A(t_0)] = [v^0{}_A(t_0)] + [v^1{}_A(t_0)] + \ldots + [v^J{}_A(t_0)] + \ldots + [v^N{}_A(t_0)] \quad (03)$$

where:

$[v_A(t_0)]$ nodal voltage vector of the network
$[v^0{}_A(t_0)]$ nodal voltage vector of the network (0)
$[v^J{}_A(t_0)]$ nodal voltage vector of the network (J)

2.2 Nonlinear inductances and resistances

As mentioned in section 2, the calculation of nodal voltages in a nonlinear network at instant t_0, requires to solve simultaneously equations (01) and (02). In this paper analytical expressions for the functions f_i (i=1,N) of the equation (02) are derived.

2.2.1 - N nonlinear inductances

The application of Faraday-Lenz's law for those inductances leads to the following matricial equation:

$$[v_{km}(t)] = \frac{d}{dt} [\lambda_{km}(t)] \quad (04)$$

where:

$v_{km}(t)$ - voltage across the node pair k-m of one nonlinear inductance
$\lambda_{km}(t)$ - flux through nonlinear inductance between node pair k-m

Using the trapezoidal rule of integration on equation (04):

$$[\lambda_{km}(t_0)] = \frac{\Delta t}{2} [v_{km}(t_0)] + [b(t_0 - \Delta t)] \quad (05)$$

where:

$$[b(t_0 - \Delta t)] = [\lambda_{km}(t_0 - \Delta t)] + \frac{\Delta t}{2} [v_{km}(t_0 - \Delta t)] \quad (06)$$

From the curve λ x i of the inductance, defined point-by-point, are derived the real parameters α_{km} and a_{km} of the equation (07) that best fit the mentioned curve.

$$i_{km} = \left[\frac{|\lambda_{km}|}{a_{km}} \right]^{\alpha_{km}} . \text{sign}(\lambda_{km}) \quad (07)$$

In equation (07) the following simplifying assumptions were made:
- hysteresis is ignored
- the curve λ x i has the following symmetry:

$$i_{km}(\lambda_{km}) = - i_{km}(-\lambda_{km})$$

For a set of N nonlinear inductances the equation (07) becomes:

$$[i_{km}] = \left[\left[\frac{|\lambda_{km}|}{a_{km}} \right]^{\alpha_{km}} . \text{sign}(\lambda_{km}) \right] \quad (08)$$

The equation (01) can be rewritten as:

$$[v_{km}(t_0)] = [v^0{}_{km}(t_0)] - [R_{TH}] . [i_{km}(t_0)] \quad (09)$$

Equations (05), (06), (08) and (09) lead to:

$$[F(v_{km}(t_0))] = [F(v_{km})] = [O] \quad (10)$$

This matricial equation represents a set of N nonlinear equations whose N unknown variables are the branch voltages across

nonlinear elements.The application of Newton-Raphson method produce the following iterative process:

$$[v_{km}^{(h+1)}] = [v_{km}^{(h)}] + [\Delta v_{km}^{(h)}] \qquad (11)$$

$$[\Delta v_{km}^{(h)}] = - [J^{(h)}]^{-1} . [F (v_{km}^{(h)})] \qquad (12)$$

where:

h iteration number

$$[J^{(h)}] = \frac{\partial [F (v_{km})]}{\partial [v_{km}]} \Bigg| \quad [v_{km}] = [v_{km}^{(h)}]$$

Jacobian matrix

2.2.2 - M nonlinear inductances and N-M nonlinear resistances

For the M nonlinear inductances, equations (05), (06) and (08) are used.

From the curve v x i of the resistances, defined point-by-point, the real parameters β_{km} and b_{km} of equation (13) that best fit the mentioned curve are derived.

$$i_{km} = \left[\frac{| v_{km} |}{b_{km}} \right]^{\beta_{km}} . \text{sign} (v_{km}) \qquad (13)$$

The curve v x i has the following symmetry:

$$i_{km} (v_{km}) = - i_{km} (-v_{km})$$

For a set of N-M nonlinear resistances the equation (13) becomes:

$$[i_{km}] = \left[\left[\frac{| v_{km} |}{b_{km}} \right]^{\beta_{km}} . \text{sign} (v_{km}) \right] \qquad (14)$$

Equations (05), (06), (08), (09) and (14) produce a matricial equation, which is similar to (10) and the iterative process described above (11), (12) can be applied to it.

A subroutine program called NONLIN, in Fortran 77 Language, was developed for the formulation outlined above and added to the EFEI's Electromagnetic Transients Program (Escola Federal de Engenharia de Itajuba, Brazil) under supervision of Dr.H.Dommel.

3. CASE STUDIES

In this section the following studies in a power system were realized:

- temporary overvoltages that led to saturation a power transformer
- switching overvoltages due to the energization of transmission line

The diferent studies were realized using subroutine NONLIN as well as other models for nonlinear elements available in EFEI's electromagentic transient program.

A comparison between the results obtained with different models in all the cases is made with the purpose of evaluate NONLIN subroutine.

Figure 4 shows the power network configuration, voltage rating 345 kV.

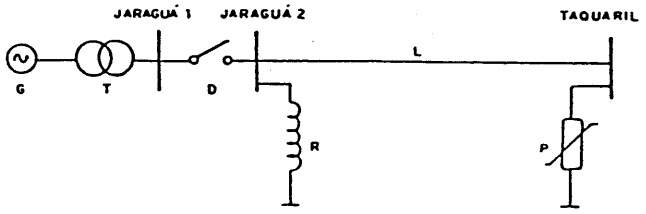

Figure 4 - Power network configuration

A brief description is made of how each element of the power system in Figure 4 was represented.

- Thevenin equivalent circuit seen from Jaguará 1 bus-bar was used to represent the generator (G) and the transformer (T).
- A reactance matrix obtained from sequence reactances data, was used to represent the shunt reactor (R).
- Transmission line (L) was simulated using the distributed parameter model.
- ZnO surge arresters (P) were represented through the characteristic v x i, as indicated in Table I.

Table I - ZnO surge arrester's curve

v(kV)	i(kA)
607.0	1.0
628.0	2.0
643.0	3.0

- Three resistances in parallel with three nonlinear inductances were added in Jaguará 1 terminal to represent λ x i curve and iron-core losses.

The data for the elements of the network were obtained of the references [7] and [8] with exception of the surge arresters.

3.1 Temporary overvoltages

Temporary overvoltages were calculated in the system (showed in Figure 4) after the energization of line (L) from sending end Jaguará with receiving end Taquaril unloaded.

In the simulations the following values were adopted:
- Thevenin's source module equal to 1.0 p.u.
- time step equal to 85 microseconds
- simulation time equal to 5 cycles

Three studies were made.The difference between them is the way to represent nonlinear inductors.

Case 1 - Nonlinear inductors were represented with "piecewise-linear" model with two slopes.

Case 2 - Nonlinear inductors were represented with "piecewise-linear" model with five slopes.

Case 3 - Nonlinear inductors were represented through NONLIN subroutine.

This last case was divided into two because two approximations of λ x i curve (from equation 07) were found.

Parameter values "α" and "a" for each functions, obtained with APROX [1] program, are indicated in Table II:

Table II - Parameter values of α and a

	α	a
NONLIN (Case 3A)	22.62809	707.0945
NONLIN (Case 3B)	23.24614	708.3523

Figures 5 and 6 show the graphics of the two approximation functions, where I and IAPROX are real and aproximate curves, respectively.

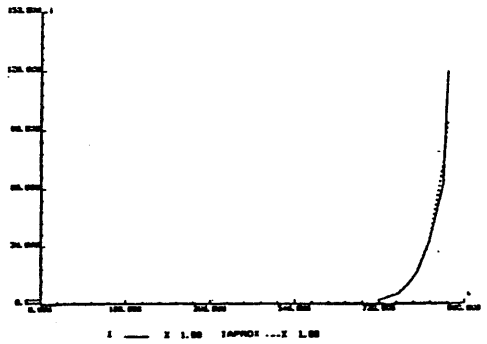

Figure 5 - Real and approximate curves for Case 3A

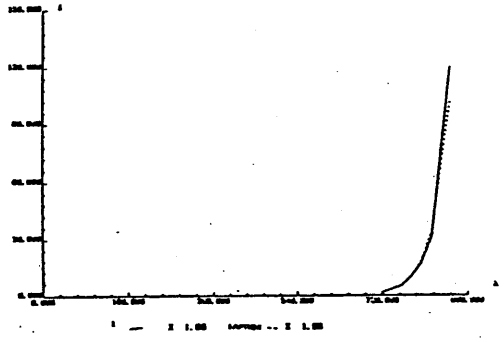

Figure 6 - Real and approximate curves for Case 3B

Maximum and minimum values of line to ground voltage in Jaguará and Taquaril bus-bars for the cases mentioned above are presented in Tables III and IV.

Table III - Voltages in Jaguará terminal

JAGUARA	Maximum (kV)	Minimum (kV)
Case 1	357.8	-363.7
Case 2	355.4	-360.1
Case 3A	361.7	-369.2
Case 3B	365.5	-373.7
Field Test [7]	364.0	-360.0

Table IV - Voltages in Taquaril terminal

TAQUARIL	Maximum (kV)	Minimum (kV)
Case 1	410.5	-410.9
Case 2	417.4	-427.8
Case 3A	420.1	-426.7
Case 3B	424.4	-431.4
Field Test [7]	419.0	-414.0

Figures 7 to 10 show line to ground voltages (phase B) in Jaguará and Taquaril bus-bars obtained from simulations for cases 2 and 3A, respectively.
Figures 11 and 12 show line to ground voltages (phase B) in the same terminals obtained from [7].

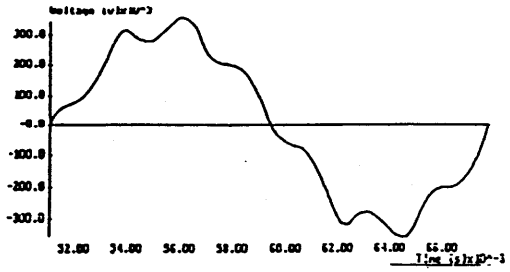

Figure 7 - Line to ground voltage (phase B) in Jaguará terminal from Case 2

Figure 8 - Line to ground voltage (phase B) in Taquaril terminal from Case 2

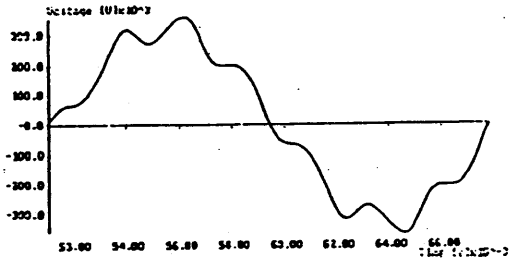

Figure 9 - Line to ground voltage (phase B) in Jaguará terminal from Case 3A

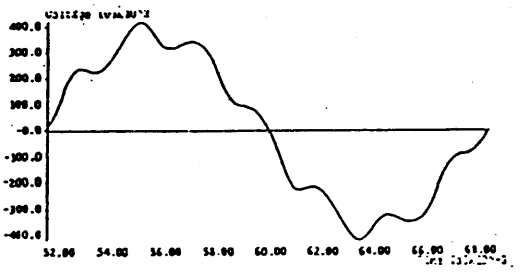

Figure 10 - Line to ground voltage (phase B) in Taquaril terminal from Case 3A

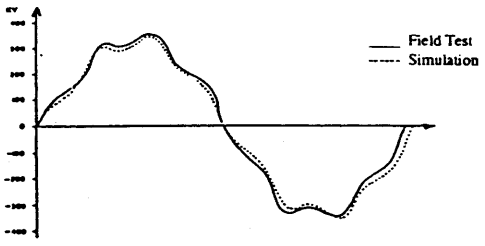

Figure 11 - Line to ground voltage (phase B) in Jaguará terminal from field test [7]

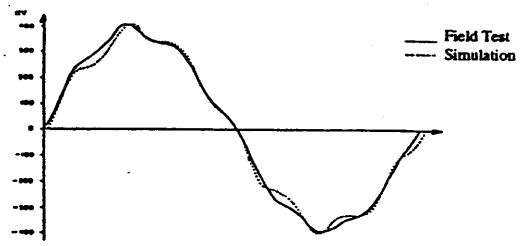

Figure 12 - Line to ground voltage (phase B) in Taquaril terminal from field test [7]

From the results obtained it can be concluded that :
- the shapes of the curves obtained from simulations are very similar particularly for cases 2, 3A and 3B
- At instant t the differences between simulations values are small, approximately 5%
- the curves, as well as maximum and minimum values from simulations, have a good agreement with field tests data.

3.2 Switching overvoltages

Switching overvoltages were calculated in the system (showed in Figure 4) when the energization of line (L) from sending end Jaguará with receiving end Taquaril unloaded.

In the simulations the following values were adopted:
- Thevenin's source module equal to 0.95 p.u.
- time step equal to 50 microseconds
- simulation time equal to 1.5 cycles

The following deterministic studies were made, in which the closing times of the circuit breakers were obtained from [7]:

Case 1 - ZnO surge arresters (P) were not represented and nonlinear inductances were represented with "piecewise-linear" model with five slopes.

Case 2 - ZnO surge arresters (P) were not represented and nonlinear inductances were represented through NONLIN subroutine.

Case 3 - ZnO surge arresters were model through CONNEC (*) and nonlinear inductors were represented through "piecewise-linear" model with five slopes.

Case 4 - ZnO surge arresters and nonlinear inductors were represented through NONLIN subroutine.

Parameters values α, a, β and b for the characteristics curves λ x i and v x i respectively were obtained with APROX program [1]. They are indicated in Table V:

Table V - α, a, β and b parameters values

α	a	β	b
19.61768	699.4287	19.16011	422999.8

In tables VI and VII are presented maximum and minimum values of line to ground voltage in Taquaril bus-bar for the cases 1 and 2.

Table VI - Maximum voltage in Taquaril terminal

Maximum (kV)	PHASE A	PHASE B	PHASE C
Case 1	288.20	512.13	604.11
Case 2	288.33	513.28	607.80
Field Test[7]	258.25	449.56	------

Table VII - Minimum voltage in Taquaril terminal

Minimum (kV)	PHASE A	PHASE B	PHASE C
Case 1	-530.19	-373.16	-398.44
Case 2	-531.44	-371.01	-398.44
Field Test[7]	-516.51	-------	-382.60

Figures 13 and 14 show line to ground voltages in Taquaril bus-bar obtained from simulations for cases 1 and 2, respectively. Figure 15 shows line ground voltages in the same terminal obtained from reference [7].

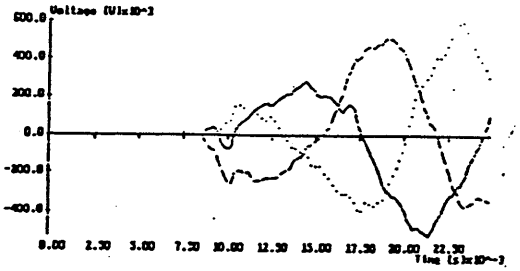

Figure 13 - Line to ground voltages in Taquaril terminal from Case 1

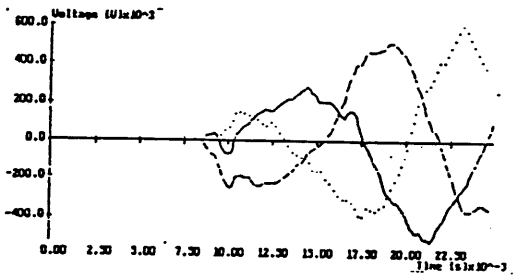

Figure 14 - Line to ground voltages in Taquaril terminal from Case 2

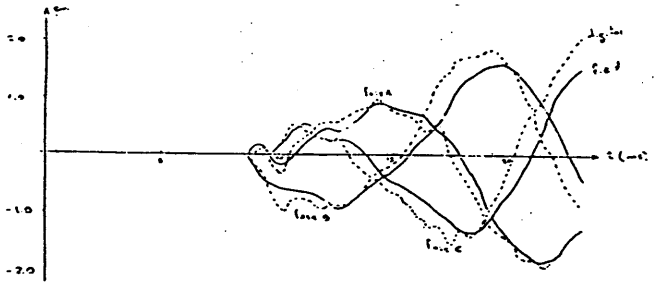

Figure 15 - Line to ground voltages in Taquaril terminal obtained from field test [7]

From the results obtained it can be concluded that :
- the shapes of the curves obtained from simulations are very similar
- at instant t the differences between simulations values are small, approximately 5%
- there are some differences between the values from simulations and from field test data. Reference [7] stated that the measurements were affected by the difficulty of calibration of the metering installation.

(*) This subroutine models ZnO surge arresters and has been incorporated to the EFEI's electromagnetic transient program

Maximum and minimum values of line to ground voltage in Taquaril bus-bar for the cases 3 and 4 are presented in Tables VIII and IX.

Table VIII- Maximum voltage in Taquaril terminal

Maximum (kV)	PHASE A	PHASE B	PHASE C
Case 3	288.20	501.21	548.48
Case 4	288.33	502.02	549.60

Table IX - Minimum voltage in Taquaril terminal

Maximum (kV)	PHASE A	PHASE B	PHASE C
Case 3	-513.19	-374.54	-398.40
Case 4	-513.96	-369.23	-397.65

In Table X are presented for these studies the maximum absolute values of surge arrester's currents.

Table X - Maximum currents through surge arresters

Maximum (A)	PHASE A	PHASE B	PHASE C
Case 3	40.62	25.81	145.11
Case 4	41.78	26.61	150.94

Figures 16 and 17 show line to ground voltages in Taquaril bus-bar obtained from simulations for cases 3 and 4, respectively.

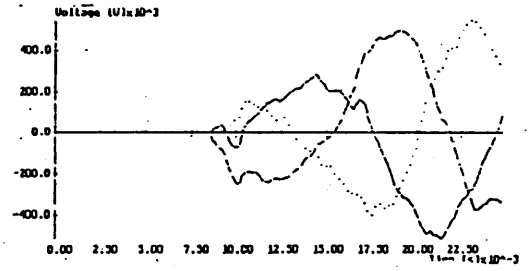

Figure 16 - Line to ground voltages in Taquaril terminal from Case 3

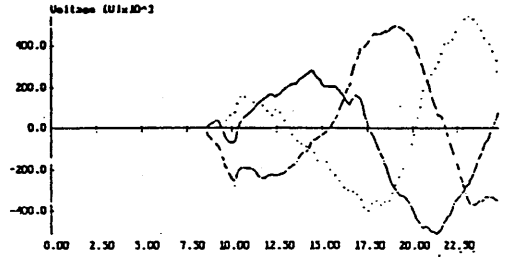

Figure 17 - Line to ground voltages in Taquaril terminal from Case 4

From the results obtained it can be concluded that :

- the shapes of the curves obtained from simulations are very similar
- at instant t the differences between simulations values are small, approximately 5%

It can be observed, comparing voltage values in Taquaril terminal from cases 3 and 4 with cases 1 and 2, that surge arresters limit switching overvoltages.

4. CONCLUSIONS

In the previous studies the NONLIN representation, had a very good behavior for switching surges and temporary overvoltages.

From the mentioned above the authors can conclude that NONLIN models of nonlinear elements are a good alternative to others models availables in EMTP and ATP programs.

5. REFERENCES

[1] - G.Calzolari.- "A Análise dos Modelos de Transformadores de Potência para Estudos de Transitórios Eletromagnéticos" - Dissertação de Mestrado - EFEI - 1990.

[2] - H.W.Dommel .- "Nonlinear and Time Varying Elements in Digital Simulations of Electromagnetic Transients" - IEEE Trans. PAS Vol 90, N 6, pp 2561-2567, Nov/Dec1971 .

[3] - H.H. Skilling .- "Circuitos en Ingeniería Eléctrica"- Ed.Continental - México 1962.

[4] - W.F. Tinney - "Compensation Methods for Network Solutions by Triangular Factorization" - Proc. Power Industry Computer Applications Conference, Boston, Mass, May 24-26, 1971.

[5] - H.W. Dommel - " Electromagnetic Transients Program Reference Manual EMTP Theory Book"- 1986

[6] - H.W. Dommel, I.I. Dommel .- "Transients Program User's Manual" - University of British Columbia, Vancouver, Canada 1987.

[7] - C.Cunha e H.W. Dommel .- "Reprodução por Computador de Testes de Campo na L.T. 345 kV Jaguará-Taquaril" - Paper BH/GSP/12 apresentado no "II Seminário Nacional de Produção e Transmissão de Energia Elétrica em Belo Horizonte, Brasil, 1973.

[8] - H.W. Dommel, A. Yan, R.J. Ortiz de Marcano, A.B.Miliane .- "Case Studies for Electromagnetic Transients" - University of British Columbia, Vancouver, Canada - May 1983.